

 universität
innsbruck

Institut für Ionenphysik
und Angewandte Physik



UNIVERSITATEA
„ALEXANDRU IOAN CUZA“
din IAȘI

Spectral investigations on coaxial double transparent cathode discharges

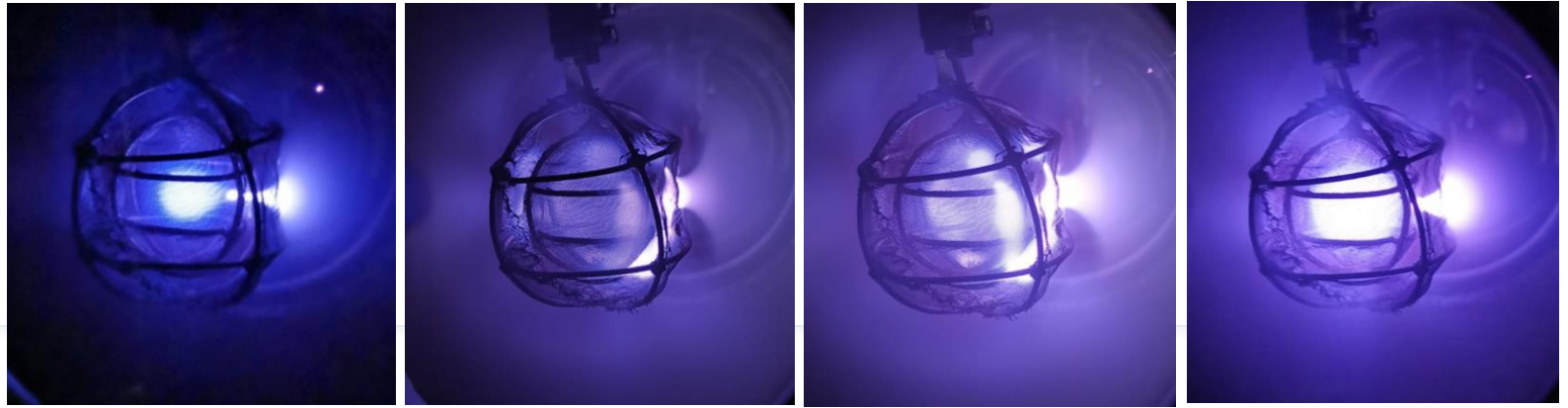
F. Enescu^{1,2}, C.T. Konrad-Soare^{1,2}, D.G. Dimitriu²,
C. Ionita¹, R.W. Schrittwieser¹

¹ *Institute for Ion Physics and Applied Physics, University of
Innsbruck, Austria*

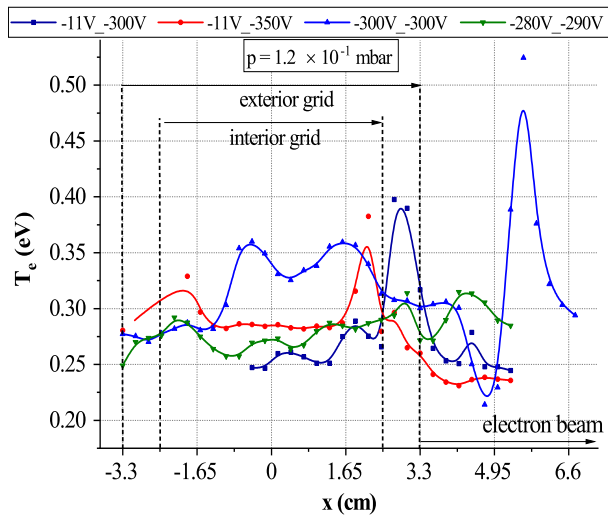
² *Faculty of Physics, Alexandru Ioan Cuza University, Iași,
Romania*

Previous experiments

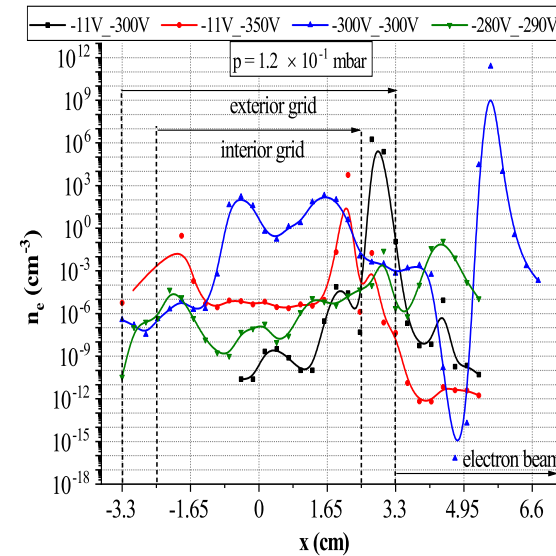
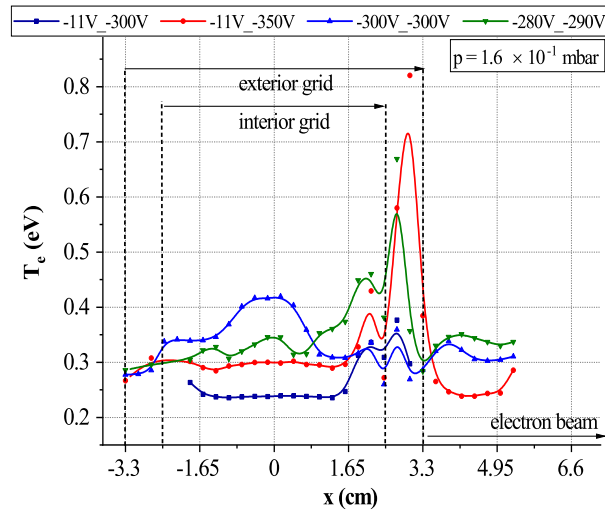
- Spectral investigations on concentric double hollow grid cathode discharges



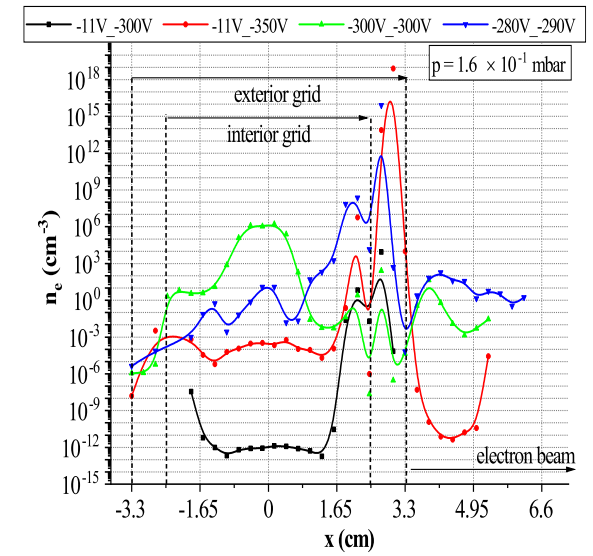
Double hollow grid discharges at $1,2 \cdot 10^{-1}$ mbar, $V_{ext} - V_{int} =$ (a) $-11V - -300V$, (b) $-11V - -350V$, (c) $-280V - -290V$ and (d) $-300V - -300V$.



Axial distribution of electron temperature



Axial distribution of electron density



New Experimental Setup With Cylindrical Electrodes

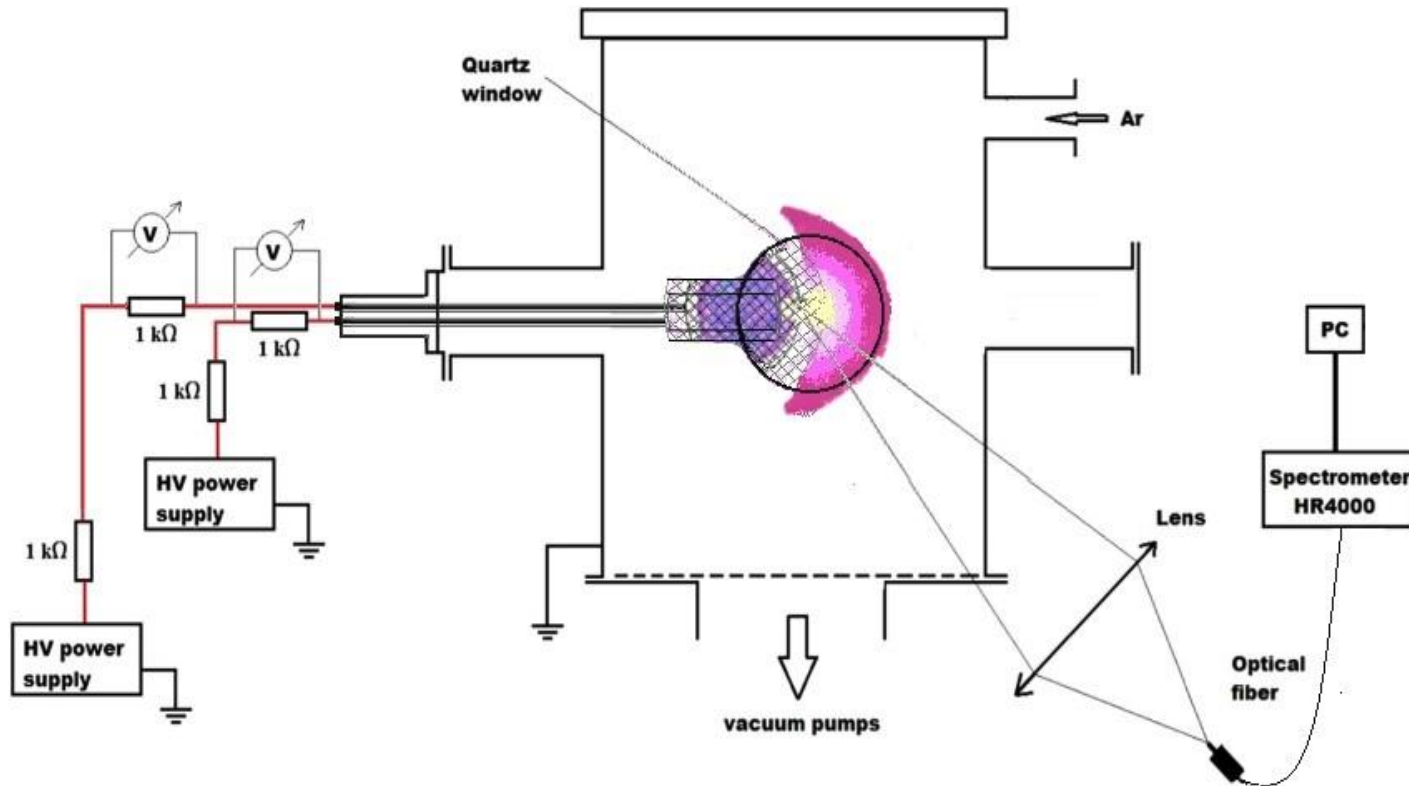
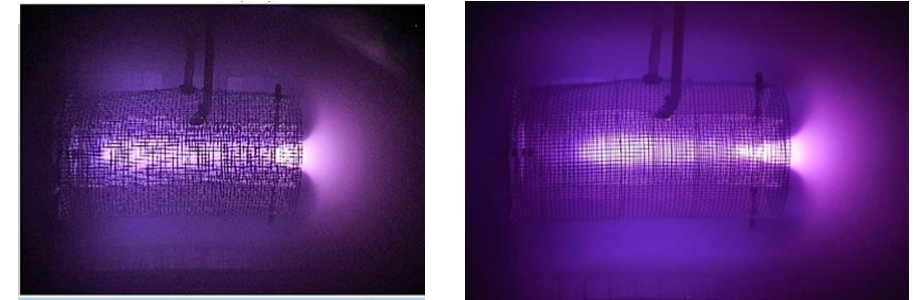


Fig. 1. Schematic of the experimental setup



- *Fig. 2. Double hollow grid discharges at $1,2 \cdot 10^{-1}$ mbar Argon, $V_{ext} - V_{int} = (a) -100V - -275V, (b) -150V - -268V$.*
- Two gridded cylinders (mesh size 1,2 x 1,2 mm, wire \varnothing 0,6 mm) cylinders with 3 and 6 cm diameter, respectively, and 10 cm length each.
- Experiments were carried out in a grounded small stainless steel cylindrical chamber of 92 cm length and 53,5 cm diameter.
- An Ocean Optics HR4000 spectrometer has been used in order to record the emission spectra of the plasma. One mm^3 of the plasma volume was focused through a lens onto an optic fiber. Axial profiles of the electron temperature and density were taken throughout the discharge.

Results

Optical emission spectroscopy is used in order to calculate the electron temperature T_e and electron density n_e in Local Thermodynamic Equilibrium (LTE) conditions. T_e is assumed equal to the excitation and the plasma temperatures, and is determined from the intensity ratio of several spectral lines belonging to the same ionization stage. Thus, accurate temperature values are obtained by extracting the average excited temperature from the Boltzmann plot slope eq. (1). The electronic density profiles have been calculated using relative intensities of the neutral atomic lines and singly charged ionic lines according to the Saha-Eggert eq. (2).

$$I_{ki} = N_0 \frac{1}{4\pi} \frac{hc}{Z(T)} \frac{A_{ki}}{\lambda} g_k \exp\left(-\frac{E_k}{kT_e}\right) \quad (1)$$

$$n_e = \frac{2g^+ A^+ \lambda^* I^*}{g^* A^* \lambda^+ I^+} \frac{(2\pi m_e k T_e)^{3/2}}{h^3} \exp\left(-\frac{E^+ - E^* + E_i}{kT_e}\right) \quad (2)$$

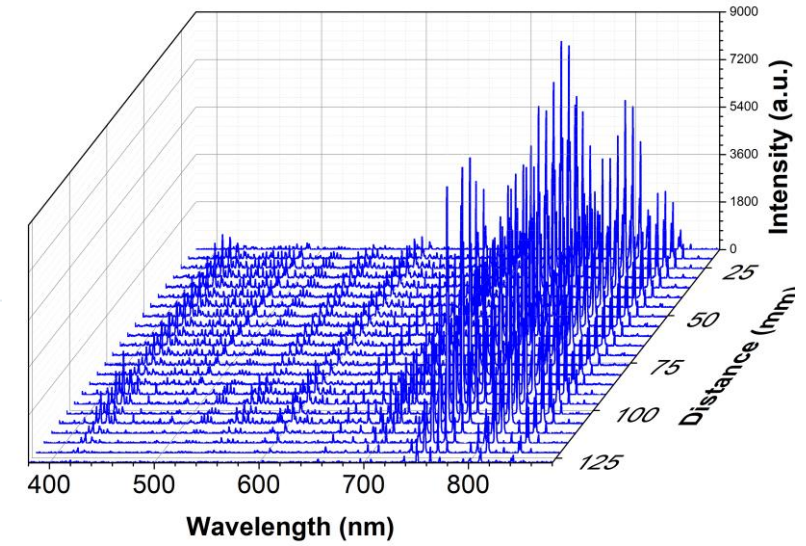


Fig. 3. Axial distribution of the plasma optical emission spectra

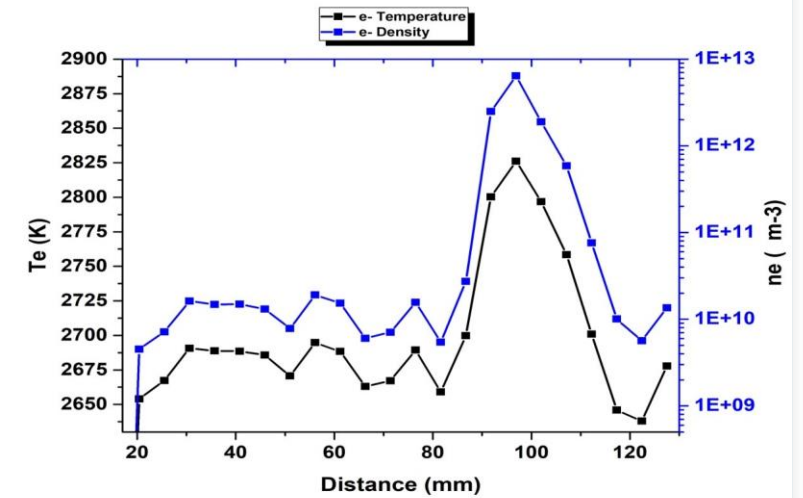


Fig. 4. Axial distribution of electron temperature and density when $V_{int} = -275$ V and $V_{ext} = -100$ V

Observations

Plasma follows the surfaces of the electrodes; they confine the plasma. Extreme biases make plasma unstable, discharges between electrodes as well as between electrodes and vacuum chamber walls appear.

The second exterior electrode inhibits the plasma structure of the inner electrode; more control over the discharges is possible by varying the potential of the outer electrode – easier to conduct the readings, more stable plasma.

We can try obtaining plasma by biasing complex shapes of electrodes and dynamic electrodes – the main issue are the measurements.

Videos and pictures of discharges,
spectacular but highly unstable discharges

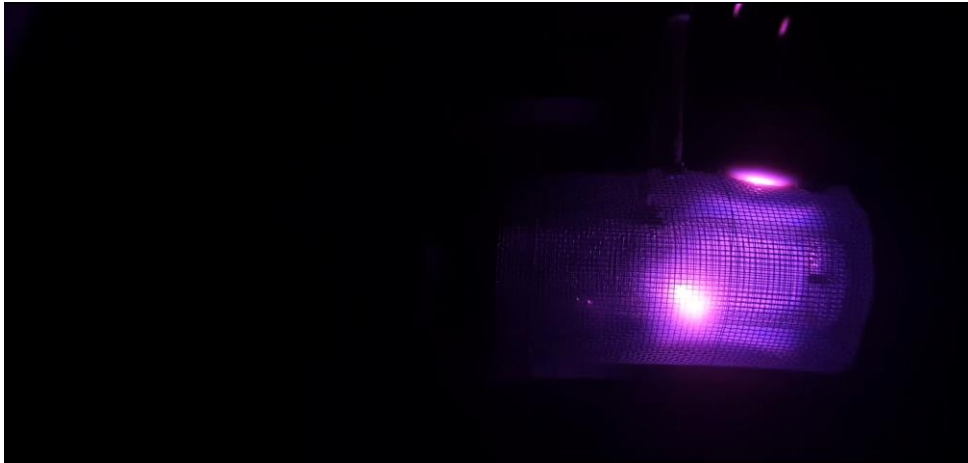


Fig. 6. Unstable discharge moving chaotically

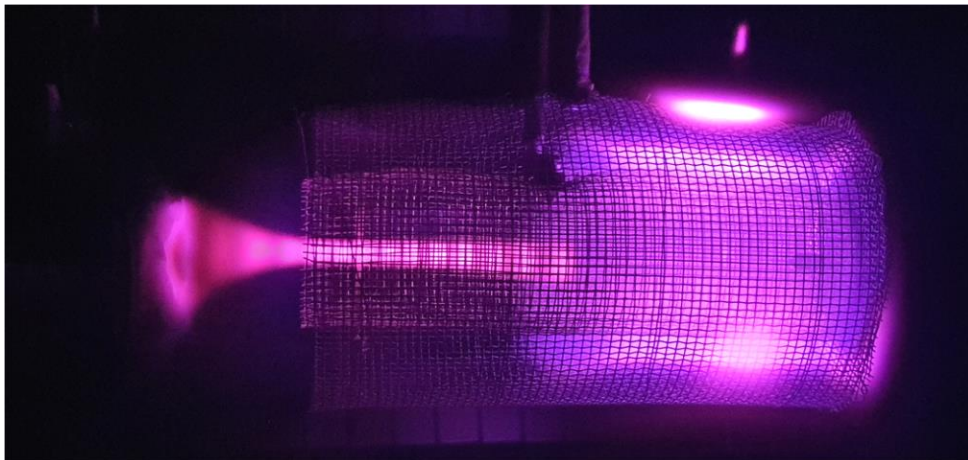


Fig. 7. Dual system spheres – cylinders, plasma discharge changing with biases

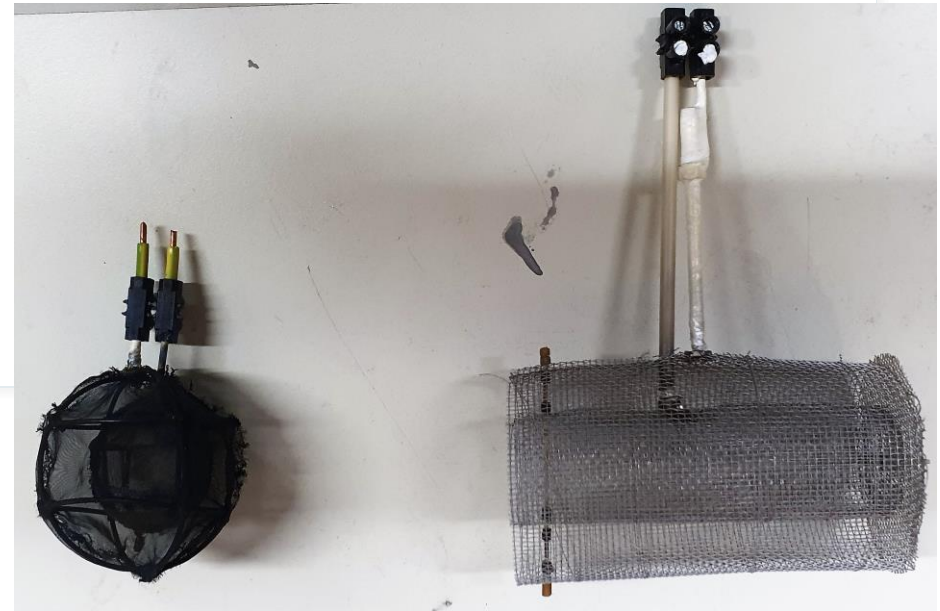
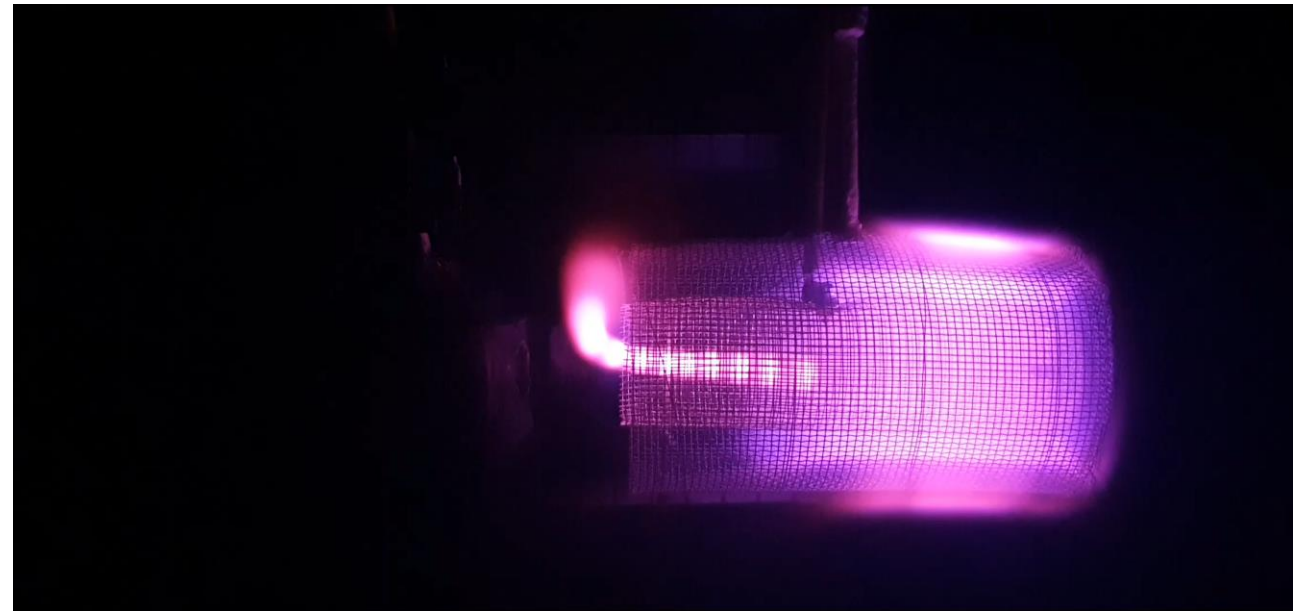


Fig. 5. The spherical and cylindrical electrodes



Future experiments

- **#1:** Future experiments involve polarizing different shapes of electrodes – in this case a Mobius band shape – and observe how plasma follows (or not) the shape of the electrode. In Fig. 5.b first we ignited the plasma discharge with a high potential, then we lowered the potential to a minimum, so the plasma fluxes were observable; in Fig. 5.a the potential was left high, the plasma followed the shape of the electrode. The challenge will be representing the data with the distance (axis of a virtual unwrapping of the Mobius electrode).

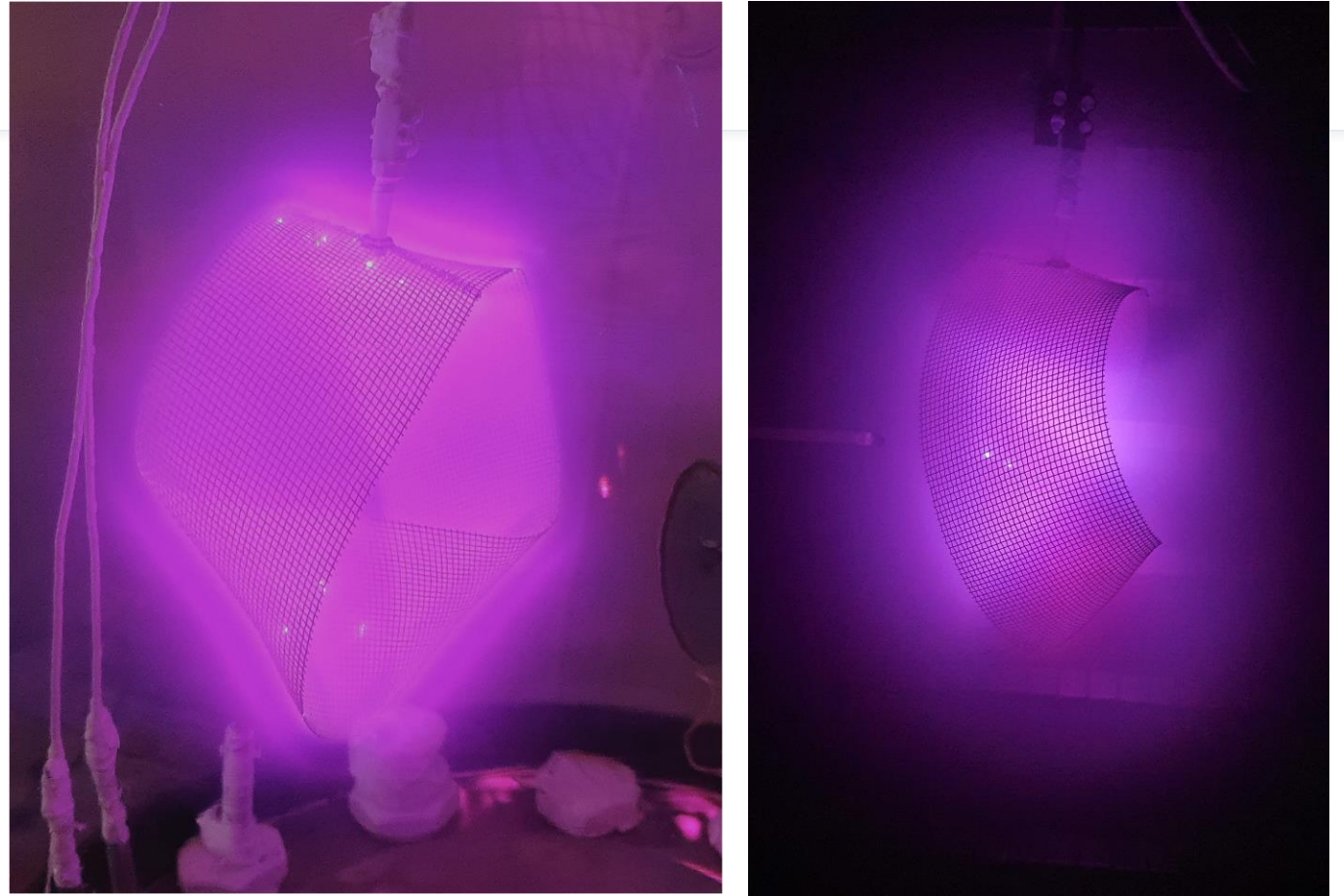
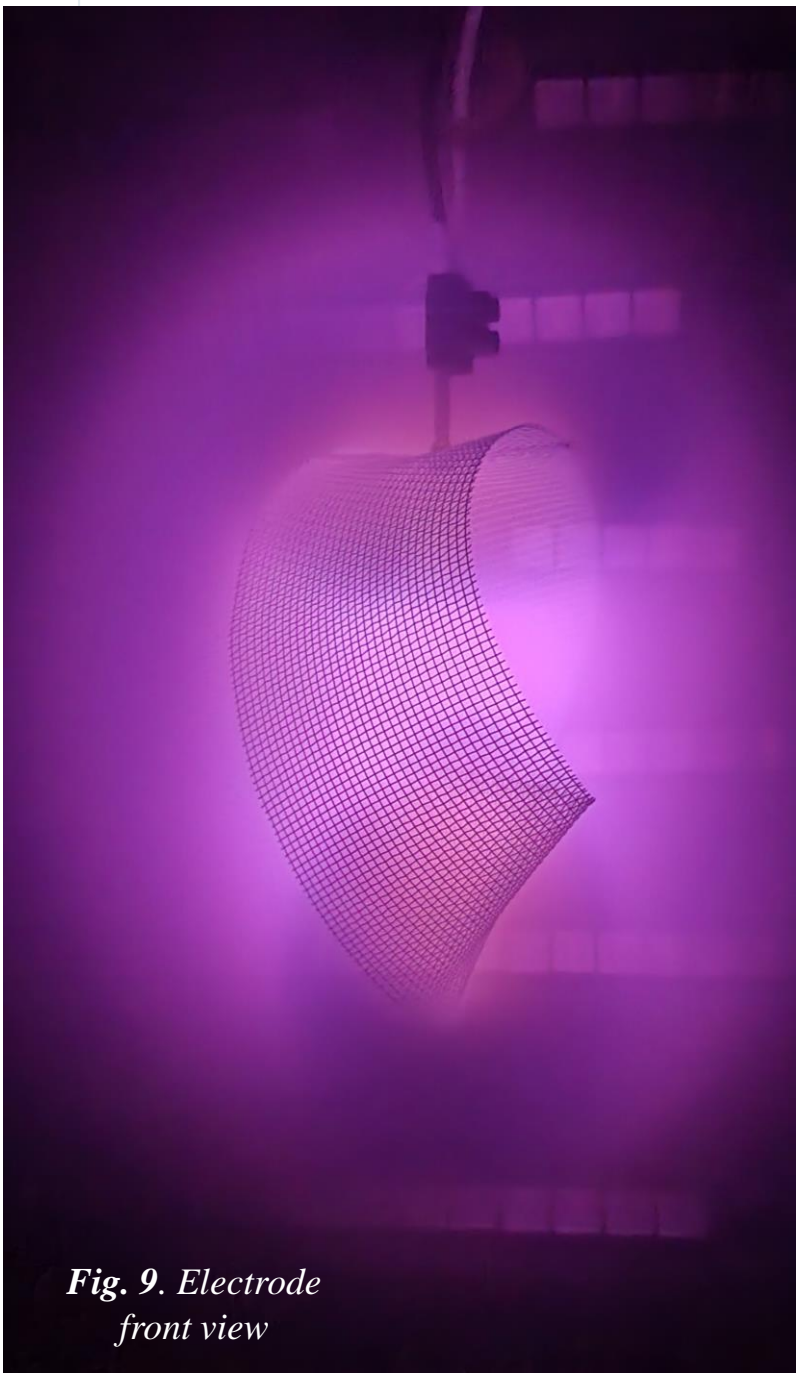


Fig. 8. Plasma discharges with a Mobius electrode. (a) UAIC – Bell shape vacuum chamber, anode at right, (b) UIBK – anode is the chamber



*Fig. 9. Electrode
front view*



*Fig. 11. Electrode in glass bell
vacuum chamber at UAIC*

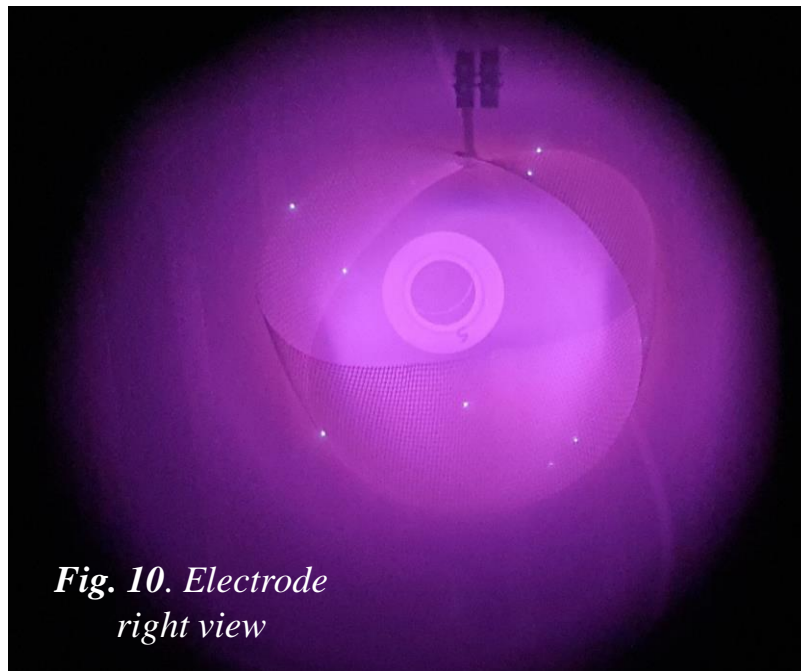


*Fig. 10. Electrode
right view*

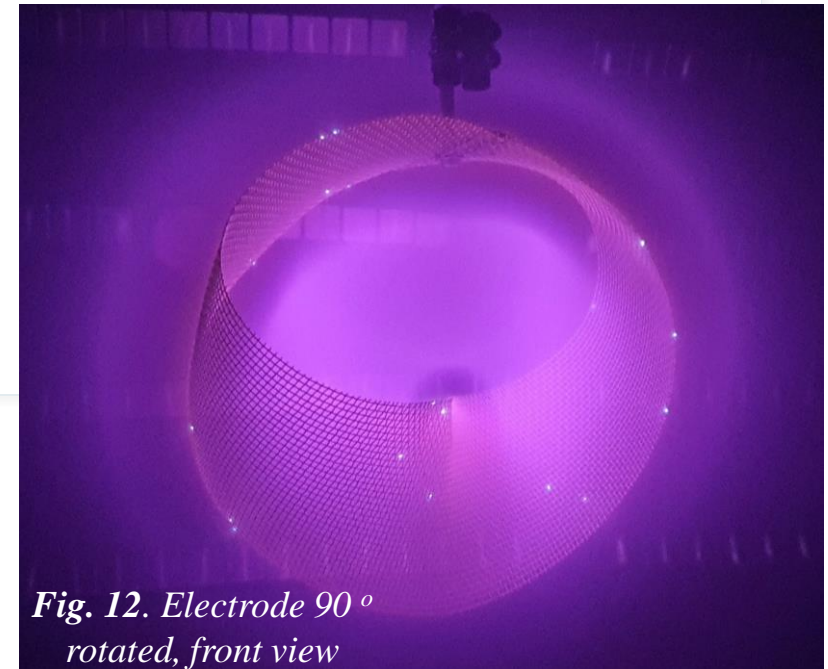


*Fig. 12. Electrode 90°
rotated, front view*

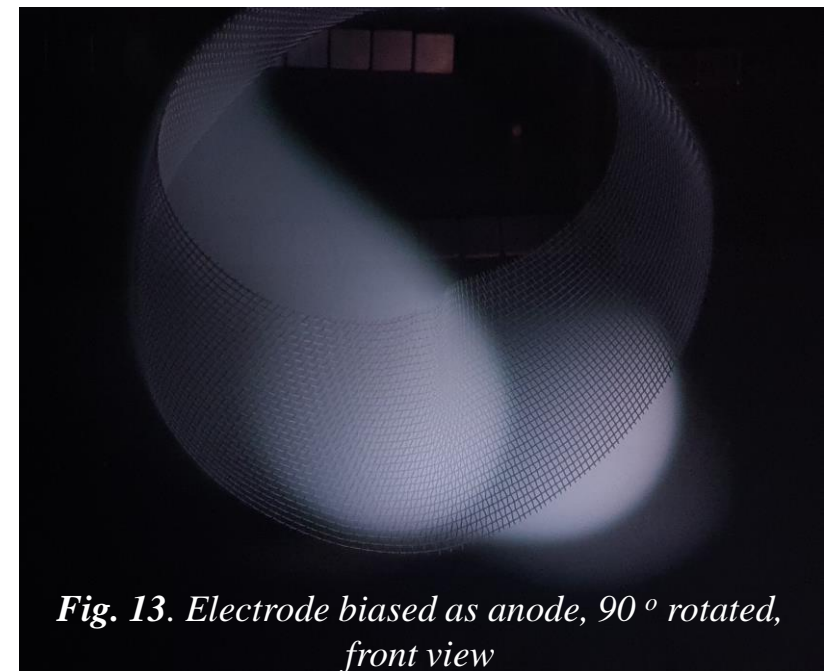


*Fig. 13. Electrode biased as anode, 90°
rotated, front view*

Future experiments

- #2. Other experiments will involve ordinary shapes in a dynamic electrode (rotating electrode, high number of rotations per minute). A dynamic electrode raises the problem of acquiring data by a (static) probe, however acquiring optical spectroscopy is still possible, the issue will be with choosing a proper reference. The mechanical stability of the system is an issue, as centrifugal forces are high, deforming the mesh, eccentricity. Lowering the rotations per minute (rpm) of the electric motor.



Fig. 15. The motor, ESC, and the spheres

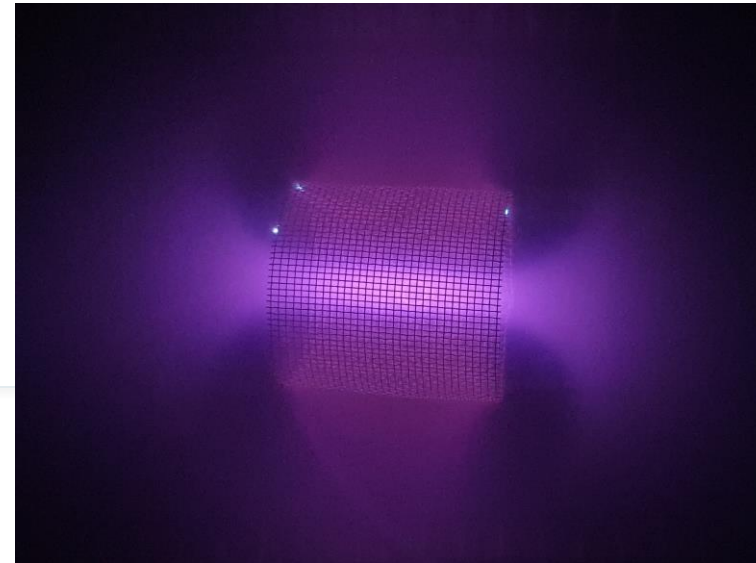


Fig. 14. Plasma discharge in a (a) static cylinder, (b) rotating cylinder.



Conclusions

- Measurements were performed in a wide range of configurations. First the primary discharge is ignited between the inner grid and the walls of the chamber, while the outer grid provides more control over the plasma structures. The volume of the discharge as well as the double layer's position are visibly affected by both the bias configuration and background pressure. Complex space charge structures can be observed in the optic axial distribution profiles of the plasma parameters, beginning with the position of the interior grid up to several cm behind the outer grid, caused by the local constraints in the electric field induced by the presence of the holes. Peak values for both electron temperature and density have been established at the open end of the cylinders.

- **References**

- [1] R. Schrittwieser et al., *Phys. Scr.* **92** (2017) 044001.
- [2] C.T. Teodorescu-Soare et al., *Int. J. Mass Spectrometry* **436** (2019) 83.
- [3] S. Gurlui et al., *Rom. J. Phys.* **54**(7–8) (2009) 705.
- [4] C.T. Teodorescu-Soare et al., *Physica Scripta* **91** (2016) 034002.
- [5] C T Konrad-Soare et al 2021 *Plasma Sources Sci. Technol.* 30 085006

Acknowledgement

This work was supported by the CEEPUS network AT-0063.